THE PERTURBATIVE RESUMMED SERIES FOR TOP PRODUCTION*

Edmond L. Berger and Harry Contopanagos
High Energy Physics Division
Argonne National Laboratory
Argonne, IL 60439

Abstract

Our calculation of the total cross section for inclusive production of $t\bar{t}$ pairs in hadron collisions is summarized. The principal ingredient of this calculation is resummation of the universal leading-logarithm effects of gluon radiation to all orders in the quantum chromodynamics coupling strength, restricted to the region of phase space that is manifestly perturbative. We present predictions of the physical cross section as a function of top quark mass in protonantiproton reactions at center-of-mass energies of 1.8 and 2.0 TeV.

1. Introduction

In this report we summarize our calculation of the inclusive cross section for top quark production¹. In hadron interactions at collider energies, the main production mechanisms for top-antitop quark $(t\bar{t})$ pair production, as modeled in perturbative quantum chromodynamics (pQCD), involve parton-parton collisions. The gluonic radiative corrections to the lowest-order channels create large enhancements of the partonic cross sections near the top pair production threshold². The magnitude of the $\mathcal{O}(\alpha_s^3)$ corrections implies that fixed-order perturbation theory will not necessarily provide reliable quantitative predictions for $t\bar{t}$ pair production at Fermilab Tevatron energies. A resummation of the effects of gluon radiation to all orders in perturbation theory is called for in order to improve the reliability of the theory. ^{3,1}.

We use the notation $\alpha(\mu) \equiv \alpha_s(\mu)/\pi$, where μ is the common renormalization/factorization scale of the problem. Unless otherwise specified, $\alpha \equiv \alpha(\mu = m)$ where m is the mass of the top quark. For the subprocess

$$i(k_1) + j(k_2) \to t(p_1) + \bar{t}(p_2) + g(k),$$
 (1)

^{*}Presented by H. Contopanagos at the XXXI Rencontres de Moriond, "QCD and High Energy Hadronic Interactions", March 23-30, 1996, Les Arcs, France

we use the partonic invariants³

$$s = (k_1 + k_2)^2$$
, $t_1 = (k_2 - p_2)^2 - m^2$, $u_1 = (k_1 - p_2)^2 - m^2$, $(1 - z)m^2 = s + t_1 + u_1$. (2)

Through next-to-leading order (NLO), keeping only the leading logarithmic contributions, we write the total partonic cross section in the $\overline{\rm MS}$ scheme as

$$\sigma_{ij}^{(0+1)}(\eta, m^2) = \int_{1-4(1+\eta)+4\sqrt{1+\eta}}^{1} dz \left\{ 1 + \alpha 2C_{ij} \ln^2(1-z) \right\} \sigma_{ij}'(\eta, z, m^2) , \qquad (3)$$

where $\eta = s/(4m^2) - 1$, $C_{ij} = C_F = 4/3$ ($C_{ij} = C_A = 3$) for $ij \equiv q\bar{q}$ (gg), $\sigma'_{ij}(\eta, z, m^2) \equiv \frac{d}{dz}\bar{\sigma}^B_{ij}(\eta, z, m^2)$, and $\bar{\sigma}^B_{ij}$ is the unpolarized Born partonic cross section. We invoke universality with the Drell-Yan case ($l\bar{l}$ production). Because the finite-order leading logarithms are identical in the $t\bar{t}$ and $l\bar{l}$ cases, we can resum them in $t\bar{t}$ -production with the same function we use in the Drell-Yan case. We find

$$\sigma_{ij}(\eta, m^2) = \int_{1-4(1+\eta)+4\sqrt{1+\eta}}^{1} dz \mathcal{H}(z, \alpha) \sigma'_{ij}(\eta, z, m^2) . \tag{4}$$

The kernel of the hard part is⁴

$$\mathcal{H}(z,\alpha) = 1 + \int_0^{\ln(\frac{1}{1-z})} dx e^{E(x,\alpha)} \sum_{j=0}^\infty Q_j(x,\alpha) .$$
 (5)

The kernel in Eq. (5) depends solely on the resummation exponent $E(x, \alpha)$, either explicitly, or through the functions Q_j which depend exclusively on E.

2. The Resummation Exponent

For the Drell-Yan process, the exponent in moment space⁵ in the Principal Value Resummation (PVR) approach⁴ may be written in the $\overline{\rm MS}$ factorization scheme as

$$E(x,\alpha) = -g^{(1)} \int_{P} d\zeta \frac{\zeta^{n-1} - 1}{1 - \zeta} \int_{(1-\zeta)^2}^{1} \frac{d\lambda}{\lambda} \frac{\alpha}{1 + \alpha b_2 \ln \lambda} . \tag{6}$$

Here P is a principal-value contour⁴ and $g^{(1)} = 2C_{ij}$. It is important to note that Eq. (6) can include in general all large logarithmic structures in the Drell-Yan case. It has a perturbative asymptotic representation⁴

$$E(x,\alpha) \simeq E(x,\alpha,N(t)) = g^{(1)} \sum_{\rho=1}^{N(t)+1} \alpha^{\rho} \sum_{j=0}^{\rho+1} s_{j,\rho} x^{j}$$
, (7)

where

$$s_{j,\rho} = -b_2^{\rho-1} (-1)^{\rho+j} 2^{\rho} c_{\rho+1-j} (\rho-1)! / j!, \tag{8}$$

and $\Gamma(1+z) = \sum_{k=0}^{\infty} c_k z^k$, where Γ is the Euler gamma function. This representation is valid in the moment-space interval

$$1 < x \equiv \ln n < t. \tag{9}$$

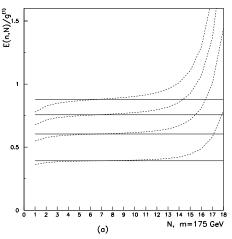
This range of validity has the consequence that terms in the exponent of the form $\alpha^k \ln^k n$ are of order unity, and terms with fewer powers of logarithms, $\alpha^k \ln^{k-m} n$, are negligible. This explains why resummation is completed in a finite number of steps. In addition, we discard monomials $\alpha^k \ln^k n$ in the exponent because of the restricted universality between the $t\bar{t}$ and $l\bar{l}$ processes. The exponent we use in our calculations is the truncation

$$E(x, \alpha, N) = g^{(1)} \sum_{\rho=1}^{N(t)+1} \alpha^{\rho} s_{\rho} x^{\rho+1},$$
(10)

with the coefficients $s_{\rho} \equiv s_{\rho+1,\rho} = b_2^{\rho-1} 2^{\rho}/\rho(\rho+1)$. The number of perturbative terms N(t) in Eq. (7) is obtained by optimizing the asymptotic approximation $\left| E(x,\alpha) - E(x,\alpha,N(t)) \right| =$ minimum. An excellent numerical approximation is provided by the fit $N(t) \simeq [t-3/2]$, where the integer part is defined as the closest integer from either direction. Throughout this paper, we use the two-loop formula for the fixed coupling strength $\alpha(m)$.

In Fig. 1a we illustrate the validity of the asymptotic approximation for a value of t corresponding to m = 175 GeV. Optimization works perfectly, with N(t) = 6, and the plot demonstrates the typical breakdown of the asymptotic approximation if N were to increase beyond N(t). This is the exponential rise of the infrared (IR) renormalons, the $(\rho-1)!$ growth in the second term of Eq. (8). As long as n is in the interval of Eq. (9), all the members of the family in n are optimized at the same N(t), showing that the optimum number of perturbative terms is a function of t only.

It is valuable to stress that we can derive the perturbative expressions, Eqs. (7), (8) and (9), without the PVR prescription, although with less certitude. We begin with the unregularized form of Eq. (6), i.e., with the integral over x on the real axis. Expanding the inner integrand as a Taylor series around α , we find the same result as Eq. (7), the only and major difference being that we do not know the asymptotic properties of this series in the full range of moments n. For a fixed t and n, one may use the monotonicity behavior of the corresponding partial sums to try to determine an upper limit for the number of terms in Eq. (7). This procedure is illustrated in Fig. 1b for m = 175 GeV. We note that beyond a certain range of N, the



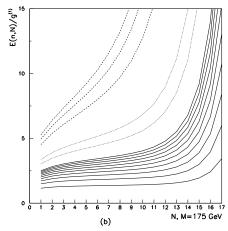


Fig. 1. Optimum number of perturbative terms in the exponent (a) with PVR (solid family is for PVR, dashed for perturbative approximation, both families increasing, for parametric values n=10,20,30,40) and (b) using monotonicity of the partial sums (solid family for $n \in \{10^2,10^3\}$ in steps of 100, dotted for $n=2,3\times10^3$ and dashed for $n=1,2,3\times10^4$).

exponent increases factorially, a demonstration of both the asymptotic nature of the series and of the effect of the IR renormalons. A range of optimum N can be determined where the growth of the sum reaches a plateau, before the factorial growth sets in at large N. The plateau is centered around $N_{opt} \simeq N(t) = [t - 3/2]$, in agreement with PVR.

3. The Resummed cross section

The general form of the PVR cross section is given by Eqs. (4) and (5). The functions $Q_j(x,\alpha)$ in Eq. (5) appear during the inversion of the Mellin transform⁴ $n \leftrightarrow z$. Specification of the perturbative regime in momentum space follows from general expressions for the inversion of the Mellin transform and the meaning of the successive terms in this inversion, once their perturbative approximations are used. The functions Q_0 and Q_1 , can be calculated⁴:

$$Q_0 = \frac{1}{\pi} \sin(\pi P_1) \Gamma(1 + P_1), \quad Q_1 \simeq 2\Gamma(1 + P_1) P_2 \cos(\pi P_1) \Psi(1 + P_1) , \qquad (11)$$

where $P_k = (\partial^k/k!\partial^k x)E$ and $\Psi \equiv \Psi^{(0)}$ and $\Psi^{(k)}$ are the usual Polygamma functions. For simplicity we include in the expression for Q_1 only terms that generate corrections starting at $\mathcal{O}(\alpha)$. Q_1 contributes one less power of x than α in the integrand of Eq. (5), and it is formally subleading relative to the contribution of Q_0 . Nevertheless, from Eq. (11) we see that this suppression is not true for values of x such that $P_1(x,\alpha) \simeq 1$. We conclude that the perturbative region in momentum space is defined by the inequality constraint

$$P_1(x_z, \alpha) \le 1$$
, $x_z \equiv \ln\left(\frac{1}{1-z}\right)$. (12)

Since we intend to resum leading logarithms only, our main result for the perturbative resummed partonic cross section, denoted by $\sigma_{ij}^{R;pert}$, is

$$\sigma_{ij}^{R;pert}(\eta, m^2) = \int_{1-4(1+\eta)+4\sqrt{1+\eta}}^{z_0} dz \left[1 + \int_0^{x_z} dx e^{E(x,\alpha)} P_1(x,\alpha) \right] \sigma'_{ij}(\eta, z, m^2)
= \int_{1-4(1+\eta)+4\sqrt{1+\eta}}^{z_0} dz e^{E(x_z,\alpha)} \sigma'_{ij}(\eta, z, m^2) ,$$
(13)

where z_0 is the end-point calculated from Eq. (12). In order to achieve the best accuracy available we wish to include in our predictions as much as is known theoretically. Our "final" resummed partonic cross section can therefore be written¹

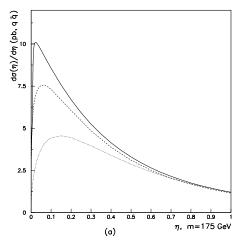
$$\sigma_{ij}^{pert}(\eta, m^2, \mu^2) = \sigma_{ij}^{R;pert}(\eta, m^2, \mu^2) - \sigma_{ij}^{(0+1)}(\eta, m^2, \mu^2) \bigg|_{R;pert} + \sigma_{ij}^{(0+1)}(\eta, m^2, \mu^2) . \tag{14}$$

The second term is the part of the partonic cross section up to one-loop that is included in the resummation, while the last term is the exact one-loop cross section².

It is useful to translate our definition of the perturbative regime directly into a statement about the perturbative region in η . Our perturbative resummation probes the threshold down to the point $\eta \geq \eta_0 = (1-z_0)/2$. Below this value, perturbation theory, resummed or otherwise, is not to be trusted. The physical cross section for each production channel is obtained through the factorization theorem.

$$\sigma_{ij}(S, m^2) = \frac{4m^2}{S} \int_0^{\frac{S}{4m^2} - 1} d\eta \Phi_{ij} \left[\frac{4m^2}{S} (1 + \eta), \mu^2 \right] \sigma_{ij}(\eta, m^2, \mu^2), \tag{15}$$

where the parton flux is $\Phi_{ij}[y,\mu^2] = \int_y^1 \frac{dx}{x} f_{i/h_1}(x,\mu^2) f_{j/h_2}(y/x,\mu^2)$. The total physical cross section is obtained after incoherent addition of the contributions from the the $q\bar{q}$ and gg production channels. We ignore the small contribution from the qg channel. We adopt one common scale μ for both the factorization and renormalization scales. A quantity of phenomenological interest is the differential cross section $\frac{d\sigma_{ij}(S,m^2,\eta)}{d\eta}$. Its integral over η is, of course, the total cross section. In Fig. 2 we plot these distributions for m=175 GeV, $\sqrt{S}=1.8$ TeV and $\mu=m$. We observe that, at the energy of the Tevatron, resummation is significant for the $q\bar{q}$ channel and less so for the gg channel. We show the total $t\bar{t}$ -production



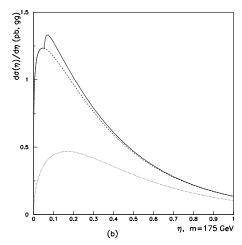


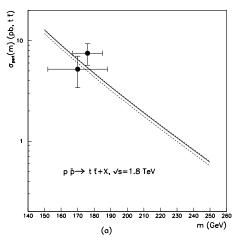
Fig. 2. Differential cross section $d\sigma/d\eta$ in the $\overline{\text{MS}}$ -scheme for the (a) $q\bar{q}$ and (b) gg channels: Born (dotted), NLO (dashed) and resummed (solid).

cross section as a function of top mass in Fig. 3. The central value of our predictions is obtained with the choice $\mu/m = 1$, and the lower and upper limits are the maximum and minimum of the cross section in the range of the hard scale $\mu/m \in \{0.5, 2\}$. Our prediction of Fig. 3a is in agreement with the data⁶. We find $\sigma^{t\bar{t}}(m = 175 \text{ GeV}, \sqrt{S} = 1.8 \text{ TeV}) = 5.52^{+0.07}_{-0.42} \ pb$. In Fig. 3b we present our predictions for an upgraded Tevatron operating at $\sqrt{S} = 2 \text{ TeV}$. Our cross section is larger than the NLO one by about 9%. We predict $\sigma^{t\bar{t}}(m = 175 \text{ GeV}, \sqrt{S} = 2 \text{ TeV}) = 7.56^{+0.10}_{-0.55} \ pb$. Over the range $\mu/m \in \{0.5, 2\}$, the band of variation of the strong coupling strength α_s is a generous $\pm 10\%$ at m = 175 GeV.

$\sigma_{q\bar{q}}(m=150 \text{ GeV; DIS})$	$\mu/m = 0.5$	$\mu/m = 1$	$\mu/m=2$
NLO	9.42	9.31	8.57
$\sigma^{pert}_{qar{q}}$	9.76	9.92	9.31
$LSvN(\mu_0 = 0.1m)$	7.9	10.0	9.7
$\sigma_{gg}(m = 150 \text{ GeV}; \overline{\text{MS}})$	$\mu/m = 0.5$	$\mu/m = 1$	$\mu/m=2$
$\frac{\sigma_{gg}(m = 150 \text{ GeV; MS})}{\text{NLO}}$	$\mu/m = 0.5$ 2.51	$\frac{\mu/m = 1}{2.22}$	$\frac{\mu/m = 2}{1.81}$
33 (, ,	. ,		. ,

Table 1. Physical cross sections in pb at $m=150~{\rm GeV}$ and $\sqrt{S}=1.8~{\rm TeV}$. The corresponding LSvN predictions are also shown, where μ_0 is their IR cutoff.

Comparing with Laenen, Smith, and vanNeerven $(LSvN)^3$, we find our central values are 10-14% larger, and our estimated theoretical uncertainty is 9-10% compared with their



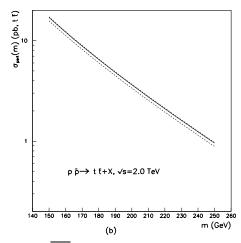


Fig. 3. Inclusive cross section for top quark production in the $\overline{\text{MS}}$ -scheme. The dashed curves show our perturbative uncertainty band, while the solid curve is our central prediction: (a) $\sqrt{S}=1.8$ TeV and (b) $\sqrt{S}=2$ TeV.

28% - 20%. Our Born cross section, however, is about 3-5% larger than the LSvN Born cross section due to the different parton distributions used in the two calculations, including differences in Λ which alone account for half or more of this increase. The two predictions have overlapping uncertainties and are, in this sense, in agreement. It is important to stress that the theoretical uncertainties are estimated in quite different ways in the two methods. We use the standard μ -variation, whereas LSvN obtain their uncertainty primarily from variations of their undetermined IR cutoffs. One of the advantages of a resummation calculation should be diminished dependence of the cross section on μ , less variation than is present in fixed-order calculations. Table 1 shows that our resummed cross sections satisfy the test of stability under variation of the hard scale μ . The resummed results show less variation than the NLO cross section. On the other hand, this is not true of the resummation of LSvN. As shown in Table 1 their $q\bar{q}$ cross section in the DIS scheme has a μ -variation of 21%. For comparison, the NLO cross section shows a variation of 9% and our resummed cross section a variation of 6%.

Scheme dependence is an extra source of theoretical uncertainty, but it should produce minimal differences for physical cross sections if these are calculated in an unambiguous resummation approach. To check for possible scheme dependent uncertainty, we perform our resummation for the dominant $q\bar{q}$ channel in both schemes. The cross sections presented in Table 2 show that our scheme dependence is insignificant, resulting in a difference of about 4% for the cross section.

m (GeV)	$\sigma_{q\bar{q}}(\mathrm{DIS};\overline{\mathrm{MS}})$	$\mu/m = 0.5$	$\mu/m=1$	$\mu/m=2$
150	NLO	9.42; 9.68	9.31; 9.53	8.57; 8.73
	$\sigma^{pert}_{qar{q}}$	9.76; 10.16	9.92; 10.42	9.31; 9.87
175	NLO	4.46; 4.54	4.39; 4.43	4.01; 4.02
	$\sigma_{qar{q}}^{pert}$	4.63; 4.78	4.69; 4.87	4.37; 4.58
200	NLO	2.20; 2.21	2.15; 2.14	1.96; 1.93
	$\sigma^{pert}_{qar{q}}$	2.29; 2.34	2.30; 2.37	2.14; 2.21

Table 2. Physical cross sections in pb for the $q\bar{q}$ channel: DIS versus $\overline{\rm MS}$ scheme.

4. Discussion and Conclusions

Our theoretical analysis shows that perturbative resummation without a model for non-perturbative behavior is both possible and advantageous. In perturbative resummation, the perturbative region of phase space is separated cleanly from the region of non-perturbative behavior. The former is the region where large threshold corrections exponentiate but behave in a way that is *perturbatively stable*. The asymptotic character of the QCD perturbative series, including large multiplicative color factors, is flat, and excursions around the optimum number of perturbative terms does not create numerical instabilities or intolerable scale-dependence. Infrared renormalons are far away from the stability plateau and, even though their presence is essential for defining this plateau, they are of no numerical consequence in the perturbative regime. Large color factors, which are multiplicative, enhance the IR renormalon effects and contribute significantly to limiting the perturbative regime.

Our resummed cross sections are about 9% above the NLO cross sections computed with the same parton distributions. The scale dependence of our cross section is fairly flat, resulting in a 9-10% theoretical uncertainty. This variation is smaller than the corresponding dependence of the NLO cross section, and it is much smaller than the corresponding dependence of the resummed cross section of LSvN. There are other perturbative uncertainties, such as dependence on parton distributions and factorization scheme, which affect our cross section minimally, at level of 4% or less. These variations are strongly correlated, so we opt not to add them in estimating the theoretical uncertainty. Commenting briefly on recent papers⁷, in which the authors state that the increase in cross section they find with their resummation method is of the order of 1% over NLO, we stand firmly by our results. As we explained there is no actual factorial growth in our expressions, of the type they suggest, precisely because we stay away from infrared renormalons in the exponent by optimizing the number of perturbative terms, and because our phase space is constrained within the perturbative regime derived by controlling the non-universal subleading logarithms. The numerical difference in the two approaches boils down to the treatment of the subleading logarithms, which can easily shift

the results by a few percent, if proper care is not taken. Our approach includes the universal leading logarithms only while theirs includes non-universal subleading structures which produce the suppression they find. In our opinion, their treatment of the subleading structures is not correct. We will present an account of these issues in a future publication.

Our theoretical analysis and the stability of our cross sections under μ variation provide confidence that our perturbative resummation procedure yields an accurate calculation of the inclusive top quark cross section at Tevatron energies and exhausts present understanding of the perturbative content of the theory. Our prediction agrees with data, within the large experimental uncertainties.

This work was supported by the US Department of Energy, Division of High Energy Physics, Contract W-31-109-ENG-38.

5. References

- E. Berger and H. Contopanagos, Phys. Lett. B361 (1995) 115 and Erratum; ANL-HEP-PR-95-82, hep-ph/9603326 (15 Mar 1996).
- P. Nason, S. Dawson and R.K. Ellis, Nucl. Phys. B303 (1988) 607; B327 (1989) 49;
 B335 (1990) 260 (E); W. Beenakker, H. Kuijif, W.L. van Neerven and J. Smith, Phys.
 Rev. D40 (1989) 54; W. Beenakker, W.L. van Neerven, R. Meng, G.A. Schuler and J.
 Smith, Nucl. Phys. B351 (1991) 507.
- E. Laenen, J. Smith and W.L. van Neerven, Nucl. Phys. B369 (1992) 543; Phys. Lett. B321 (1994) 254.
- 4. H. Contopanagos and G. Sterman, Nucl. Phys. B419 (1994) 77; B400 (1993) 211.
- G. Sterman, Nucl. Phys. B281 (1987) 310; S. Catani and L. Trentadue, Nucl. Phys. B327 (1989) 323; B353 (1991) 183; H. Contopanagos, E. Laenen and G. Sterman, hep-ph/9604313 (13 Apr 1996)
- P. Azzi (CDF collaboration); P. Bhat (D0 collaboration), Proceedings of the XXXI Rencontres de Moriond, "QCD and High Energy Hadronic Interactions", March 23-30 1996, Les Arcs, France.
- S. Catani, M. Mangano, P. Nason and L. Trentadue, hep-ph/9602208 (1 Feb 1996); hep-ph/9604351 (18 Apr 1996).